Active Vibration Reducing of a One-link Manipulator Using the State Feedback Decoupling and the First Order Sliding Mode Control

Mohammed BAKHTI [(a)] , Badr BOUOULID IDRISSI [(b)]

Ecole Nationale Supérieure d'Arts et Métiers
The University of Moulay Ismail _ Meknes
Morocco
[(a)]mdbakhti@yahoo.fr, [(b)]bbououlid@yahoo.fr,

ABSTRACT

This article presents an application of the first order sliding mode control in order to damp the mechanical vibrations of a flexible one-link manipulator using piezoceramic actuators.
The flexible manipulator, seen as a multiple inputs multiple outputs system is decoupled using state feedback scheme.
The model of the system is deduced using the finite element method, and its response to a control torque is calculated using the Lagrange equations. The state space equations are expressed in order to simplify the simulation and the controller implementation.

Keywords: flexible structure, first order sliding mode control, state feedback decoupling, piezoceramic actuators.

1. INTRODUCTION

The active control of flexible structures has been covered by a large number of research papers due to its high potential for industrial applications. For small amplitude vibration on very flexible structures, active approaches lead to lightweight and high performance control systems [1].
Used as sensors or actuators, piezoelectric materials have been well-studied [1], with [2] the first to suggest this idea.
Bailey and Hubbard [3] used distributed-parameter control theory and a piezoceramic actuator to actively control vibration on a cantilever beam actively.
Other researchers [4,5] studied the effect of the actuators on the host structures for vibration control through modal shape analysis. A variable structure adaptive controller developed by [6] to control contact forces on a cantilever beam used only the output force as feedback, resulting in undesirable chattering. Artificial neural networks (ANN) for identification and state feedback control of flexible structures have been implemented with good preliminary results [7]. Robust control focuses on the ability to have good control performance and stability in the presence of uncertainty in the system model as well as its exogenous inputs, including disturbances and noise. The H1 controller compensates for some of these uncertainties in active vibration control [8]. Recently, [9] developed a robust rejection method using a Kalman filter to estimate the system states under persistent excitation.
A large amount of research has focused on the optimization of sensors/actuators numbers and location, an example being [10]. Wang et al. [11] have very recently introduced PC for vibration suppression on a motor driven flexible beam, with very good simulation and practical results. These initial results were used also to diminish tip vibration on flexible beams [12].
The problem of decoupling linear multi-inputs multi-outputs systems has been subject of a great number of researchers works. Morgan [13] gave a sufficient condition for decoupling systems and defined a rather restrictive class of control laws which decouple. Additional results were obtained by Rekasius [14]. More recently, Falb and Wolovich [15] gave necessary and sufficient conditions for decoupling. They also restricted the class of control laws which decouple, which subsumes the classes introduced in [14] and [15]. Still more recently they obtained necessary and sufficient conditions on control laws for decoupling.
The control design methods to dominate the uncertainties and disturbances of systems have also attracted great research interest [16_18].
Among existing control strategies, the sliding mode control (SMC), first proposed in the early fifties, is one of the most suitable control design methods to dominate the uncertainties and disturbances acting on a system [19]. In the early sixties, the method has gained significant research attention, and has been widely applied in a variety of applications [18]. This technique has been applied to control a one flexible robot arm by [20].It also has been developed in association to piezoceramic actuators[21, 22].
Advantages of the SMC are robustness to parameter uncertainty, insensitivity to bounded disturbances, fast dynamic response, remarkable computational simplicity with respect to other robust control approaches and easy implementation [18].
The problem of the traditional (first-order) SMC method is mainly the problem of chattering. The chattering is due to the inclusion of the sign function in the switching term and it can cause the control input to start highly oscillating around the sliding surface, resulting in undesired actuators effects. This problem has been processed using two approaches: the first is to smoothen the switching term as the sliding surface gets closer to zero (soft switching) by using the continuous approximations of the discontinuous sign function, and the second is to generate ``higher-order sliding modes", first introduced by Levant in 1987 [23]. In first order sliding mode controller design, the sliding surface is selected such that it has relative degree one with respect to the control input. That means the control input acts on the first derivative of the sliding surface. Higher-order sliding mode is the generalization of the

first-order sliding mode and the control input is performed such that it acts on higher derivatives of the sliding surface.
This paper will present a contribution based on the association of the state feedback decoupling and the first order sliding mode control to actively damp a flexible one-link manipulator.
The one-link manipulator considered as a Bernoulli beam is modeled in section 2 using the Euler - Lagrange formulation. The proper modes of vibration are calculated based on a finite element analysis and truncated to the first two more significant modes. Piezoceramic actuators effect on the model is introduced via the stiffness and force matrices. In section 3, the formulation of the decoupling problem is presented, and the control laws to decouple are calculated. Section 4 will deal with the first order sliding mode controller implementation. Thus, the sliding surfaces will be designed, and the control laws will be expressed. Finally, results of simulation will be illustrated in section 5, and conclusions given in section 6.

2. MODELING OF THE FLEXIBLE ONE-LINK MANIPULATOR

This section deals with the modeling of the flexible one-link manipulator. A model is developed for the case of a manipulator with one flexible link constrained to acting on a horizontal plane, and which is rigidly attached at one end to the shaft of an electric servomotor.
Two reference systems are defined:
1. X-Y-Z system: An inertial system with its origin at the centre of the shaft of the actuator, its z-axis aligned with the shaft, and the x-axis aligned with the home position of the manipulator.
2. r-w-Z system: A rotating system, attached to the actuator's shaft, with its z-axis coincident with the inertial system's z-axis and its r-axis tangent to the link at the shaft.

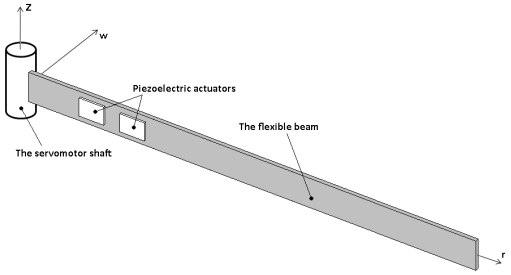

Figure 3.1: Configuration of the flexible one-link manipulator

The total displacement of the manipulator is considered to be the sum of rigid body rotation plus the flexible motion, as follows:

$$y(r,t) = \theta(t).r + w(r,t) = \theta(t).r + \sum_{i=1}^{N} a_i(t).\varphi_i(r)$$

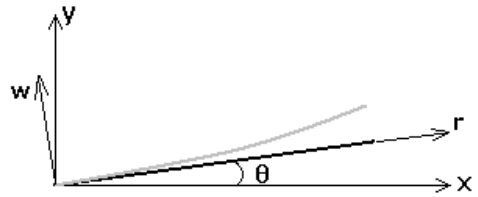

Figure 3.1: The flexible one- link manipulator displacement

The relative displacement is truncated to the first two flexible modes that have the most significant contribution to the global behavior of the system.

$$w(r,t) = a_1(t).\varphi_1(r) + a_2(t).\varphi_2(r)$$

Two layer of piezoelectric film are bonded to the manipulator in order to control the flexible modes.

2.1 Effect of the servomotor

The behavior of the link relative to the r- w -Z system can be analyzed using beam theory. Assuming that the link is a homogeneous slender beam of constant cross-section, the equations of motion can be found using the Bernoulli-Euler theory.
The flexible modes are calculated using the finite element method.
The elementary matrices of mass end stiffness are given by:

$$M = \frac{\rho sL}{420}\begin{bmatrix} 156 & 22l & 54 & -13l \\ 22l & 4l^2 & 13l & -3l^2 \\ 54 & 13l & 156 & -22l \\ -13l & -3l^2 & -22l & 4l^2 \end{bmatrix}$$

$$K = EI/l^3\begin{bmatrix} 12 & 6l & -12 & 6l \\ 6l & 4l^2 & -6l & 2l^2 \\ -12 & -6l & 12 & -6l \\ 6l & 2l^2 & -6l & 4l^2 \end{bmatrix}$$

And the analysis leads to an equation like:

$$M\ddot{q} + Kq = 0$$

The proper modes are given by the eigen vectors of the matrix: $M^{-1}K$, and the pulsations of vibration are given by the eigen values of the same matrix.

The magnitude of the velocity of any point of the link can be obtained by:

$$\dot{y}(r,t) = \dot{\theta}(t).r + \dot{w}(r,t) = \dot{\theta}(t).r + \sum_{i=1}^{2} \dot{a}_i(t).\varphi_i(r)$$

The kinetic energy of the manipulator can be written as the sum of rotational and translational components as:

$$T = \frac{J_m.\dot{\theta}(t)^2}{2} + \frac{1}{2}\int_0^L \dot{y}(r,t)^2\, dm$$

$$= \frac{J_m.\dot{\theta}(t)^2}{2} + \frac{1}{2}\int_0^L \left(\dot{\theta}(t).r + \sum_{i=1}^{2} \dot{a}_i(t).\varphi_i(r)\right)^2 \rho.S.dr$$

Where ρ is the density of the beam's material, S and I respectively its cross-sectional area and moment of inertia, and J_m is the motor fixture inertia.

The potential energy is stored in the manipulator as strain energy in the flexible link, and it can be expressed in terms of the mode shapes and modal coordinates as follows:

$$V = \frac{1}{2}EI\int_0^L \left(\frac{\partial^2 y(r,t)}{\partial r^2}\right)^2 dr$$

$$= \frac{1}{2}EI\int_0^L \left(\sum_{i=1}^{N} a_i(t).\frac{\partial^2 \varphi(r)}{\partial r^2}\right)^2 dr$$

E is the Young's modulus.

The joint angle and the modal coordinates can be grouped to form a vector of generalized coordinates, defined as:

$$q_{3\times 1} = [\theta\ a_1\ a_2]^{\mathrm{T}}$$

Similarly, the torque T applied at the joint and the modal forces can be grouped to form a vector of generalized forces.

Since there are no modal forces being applied to the system, the vector of generalized forces can be written as:

$$Q_{3\times 1} = [T\ 0\ 0]^{\mathrm{T}}$$

The work done by non-conservative external forces can then be written in terms of the generalized coordinates and forces as:

$$\mathrm{W_{nc}} = \mathrm{Q^T q} = \mathrm{T\theta}$$

Since the kinetic and potential energy are already expressed in terms of the vector of generalized coordinates, the Lagrange's equations can be expressed:

$$\frac{d}{dt}\left(\frac{\partial(T-V)}{\partial \dot{q}_i}\right) - \frac{\partial(T-V)}{\partial q_i} = Q_i \qquad i = 1 \ldots N$$

Substituting the expressions for kinetic and potential energy and performing the required operations, one obtains the following matrix equation, which is a set of 3 ordinary differential equations, that model the dynamic behavior of the system:

$$M\ddot{q} + Kq = \begin{bmatrix} k_m \\ 0 \\ 0 \\ . \\ : \\ 0 \end{bmatrix} u(t) = f.u(t)$$

Where u is the control voltage sent to the servomotor amplifier. The system matrices are given by [12]:

$$M = \begin{bmatrix} Jm + \frac{\rho S L^3}{3} & \rho S\int_0^L \varphi_1(r).r.dr & \rho S\int_0^L \varphi_2(r).r.dr \\ \rho S\int_0^L \varphi_1(r).r.dr & \rho S\int_0^L {\varphi_1}^2(r).r.dr & 0 \\ \rho S\int_0^L \varphi_2(r).r.dr & 0 & \rho S\int_0^L {\varphi_2}^2(r).r.dr \end{bmatrix}$$

$$K = \begin{bmatrix} 0 & 0 & 0 \\ 0 & EI\int_0^L \left(\frac{\partial^2 \varphi_1(r,t)}{\partial r^2}\right)^2 dr & 0 \\ 0 & 0 & EI\int_0^L \left(\frac{\partial^2 \varphi_2(r,t)}{\partial r^2}\right)^2 dr \end{bmatrix}$$

The motor and hub parameters needed for the numeric calculation of the mass and stiffness matrices are shown in Table 2.2. The link parameters are listed in Table 2.1.

Table 2.1: Link Properties

Density	ρ = 2700 Kg/m^3
Length	L = 1.1 m
Young's modulus	E = 6.9 10^{10} Pa
Cross-section area	S = 8 10^{-8} m²
The quadratic moment	I = 2.67 10^{-8} m^4

Table 2.2: Motor-Hub Properties

Motor-Fixture Inertia	J_m = 4 10^{-3} Kg m²
Friction Coefficient	B_m = 6.79 10^{-2} Nm/rad/s
Motor Constant	k_m = 1 Nm/V

The effects of actuator friction and the link structural damping can be included in the model via a viscous damping matrix given by:

$$H = \begin{bmatrix} B_m & 0 & 0 \\ 0 & 2\xi_1 m_{22}\omega_1 & 0 \\ 0 & 0 & 2\xi_2 m_{33}\omega_2 \end{bmatrix}$$

Where $\omega_i\ i = 1..2$ are the clamped-free frequencies of the link, m_{ii} are the corresponding elements of the mass matrix, and ξ_i are the modal damping coefficients.

This yields to the following modified dynamic model:

$$M\ddot{q} + H\dot{q} + Kq = k_m u$$

2.2 Effect of the piezoceramic actuators

When the piezoceramic film (PZT) is used as an actuator, its effect on the dynamic model is through the passive stiffness and the force produced by the actuator.

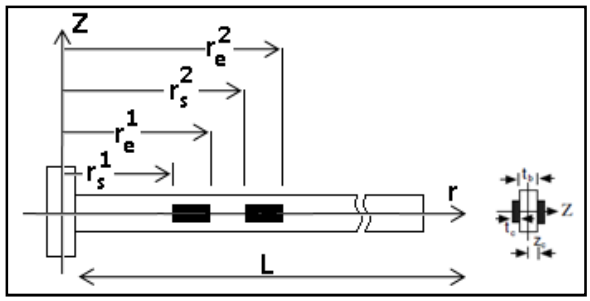

Figure 3.3: The PZT actuators setup

The contributions of the n$^{\mathrm{th}}$ PZT to the overall stiffness matrix and global force matrix are given by [24]:

$$K_{pij}^n = \frac{E_c W_c t_c t_b^2}{4}\int_{r_s^n}^{r_e^n} \left(\frac{d^2\phi_i(x)}{dx^2}\frac{d^2\phi_j(x)}{dx^2}\right) dx$$

$$F_{pi}^n = f_{pi}^n u_p^n(t)$$

Clearly, $K_{pij}^n = 0$ when i does not equal j due to the orthogonality characteristics of mode shapes. F_{pi}^n is the generalized force associated with the i$^{\mathrm{th}}$ mode. The coefficient of the generalized force is defined as:

$$f_{pi}^n = -sgn(z_c)\ \frac{d_{31}E_c W_c t_b}{2}\int_{r_s^n}^{r_e^n} \Xi_c^n \left(\frac{d^2\phi_i(x)}{dx^2}\right) dx$$

Where $u_p^n(t)$ is the voltage applied to the n$^{\mathrm{th}}$ PZT actuator.

Introducing the effect of piezoelectric films, the new system dynamic model can be described as

$$M_{ps}\ddot{q} + H_{ps}\dot{q} + K_{ps}q = f_{ps}u$$

The new modal stiffness matrix K_{ps} is a combination of matrix K and K_{pij}

$$K_{ps} = \begin{bmatrix} 0 & 0 & 0 \\ 0 & E_b I_{cs} \int_0^L \frac{d^2\phi_1(r)}{dr^2} dr + K_{p11} & 0 \\ 0 & 0 & E_b I_{cs} \int_0^L \frac{d^2\phi_2(r)}{dr^2} dr + K_{p22} \end{bmatrix}$$

Where $K_{pij} = \sum_{n=1}^{2} K_{pij}^n$ and K_{pij}^n is obtained by evaluating Eq.(12) with the parameters on nth PZT film.

The modal force coefficient matrix f_{ps} is

$$f_{ps} = \begin{bmatrix} ku & 0 & 0 \\ 0 & f_{p1}^1 & f_{p1}^2 \\ 0 & f_{p2}^1 & f_{p2}^2 \end{bmatrix}$$

Where f_{pi}^n is obtained by evaluating Eq. (14) with the parameters of nth PZT film associated with mode i.

The input voltage vector u to the motor that rotate the beam and the voltage to the PZT actuators are:

$$u = [u_m(t) \;\; u_p^1(t) \;\; u_p^2(t)]_{3\times 1}^T$$

Therefore, the system's generalized force matrix now includes two components: the force produced by the voltage applied to the motor $u_m(t)$ and the force produced by the voltage applied to the piezoelectric actuators $u_p^n(t)$(n = 1, 2).

The PZT parameters are shown in Table 2.3.

Table 2.3: Piezoceramic actuators properties and placement

Material	PZT
Application	Actuator
Charge constant d_{31} (C/N)	$175 \cdot 10^{-12}$
Capacitance C_c (F)	$2 \cdot 10^{-8}$
Young's modulus E_c (N/m2)	$6.5 \cdot 10^{10}$
Width W_c (m)	0.025
Thickness t_c (m)	$5 \cdot 10^{-4}$
Length (m)	0.025
Shape function Ξ_c	1
r_s^1 (m)	0.1
r_e^1 (m)	0.125
r_s^2 (m)	0.150
r_e^2 (m)	0.175

2.3 State Space equations formulation

For modeling and control purposes it is convenient to write the model of the system in state-space form, as follows:

$$\dot{x}(t) = Ax(t) + BQ(t)$$

Where $x = [\theta \;\; a_1 \; a_2 \;\; \dot{\theta} \;\; \dot{a}_1 \; \dot{a}_2]^T$

Matrices A and B are defined in terms of the stiffness, mass and damping matrices K_{ps}, M_{ps} and H_{ps}, respectively, and the force vector f_{ps}.

$$A = \begin{bmatrix} 0_{3\times 3} & I_{3\times 3} \\ -[M_{ps}{}^{-1}K_{ps}]_{3\times 3} & -[M_{ps}{}^{-1}H_{ps}]_{3\times 3} \end{bmatrix}_{6\times 6}$$

And $$B = \begin{bmatrix} 0_3 \\ [M_{ps}{}^{-1}f_{ps}]_3 \end{bmatrix}_{6\times 3}$$

Since the tip displacement is considered, the output vector is given by:

$$y = C.x = \begin{bmatrix} y_1(t) \\ y_2(t) \\ y_3(t) \end{bmatrix}$$

With :

$$\begin{cases} y_1(t) = L.\theta \\ y_2(t) = \varphi_1(L)a_1(t) \\ y_3(t) = \varphi_2(L)a_2(t) \end{cases}$$

So the total tip displacement is expressed as the sum of the rigid body motion plus the flexible cmodal contributions.

$$d(L,t) = L.\theta + a_1(t).\varphi_1(L) + a_2(t).\varphi_2(L)$$

L is the beam length.

Thus the matrix C is defined as follows:

$$C = \begin{bmatrix} L & 0 & 0 & 0 & 0 & 0 \\ 0 & \varphi_1(L) & 0 & 0 & 0 & 0 \\ 0 & 0 & \varphi_2(L) & 0 & 0 & 0 \end{bmatrix}$$

3. STATE FEEDBACK DECOUPLING

This section deals with the application of a feedback control in order to decouple the closed-loop system.

3.1 The decoupling method

Consider a linear dynamical system S:

$$\dot{x} = A.x + B.u$$
$$y = C.x + D.u$$

With inputs:

$$u(t) = [u_1 \;\; u_2 \;\; \dots \;\; u_m]_{1\times m}^T$$

State:

$$x(t) = [x_1 \;\; x_2 \;\; x_3 \;\; \dots \;\; x_n]^T$$

And outputs:

$$y(t) = [y_1 \;\; y_2 \;\; \dots \;\; y_m]_{1\times m}^T$$

The control law used, as originally proposed by Morgan is given by [13]:

$$u = F.x(t) + G.v(t)$$
$$= F.x(t) + G[v_1 \;\; v_2 \;\; v_3 \;\; \dots \;\; v_m]_{1\times m}^T$$

Where F and G are real, constant matrices of appropriate size, and v(t) is the new input to the closed-loop system.

The key to the solution of the decoupling problem is a canonical representation of integrator decoupled systems.

The system (S) can be decoupled if and only if the matrix given by :

$$[CB \;\; CAB \;\; CA^2B \;\; \dots \;\; CA^{n-1}B]$$

is nonsingular.

The transfer function of the decoupled system is given by:

$$H(s,F,G) = C.(I_n.s - A - B.F)^{-1}.B.G$$

Where I_n is the n×n identity matrix, and s is the Laplace transform variable.

Decoupling the system consist on computing matrices F end G in order to have H diagonal and nonsingular.

Let C_i be the i[th] row of the output matrix C, and $D_i = C_i.\mathrm{A}^{\mathrm{d_i}}.\mathrm{B}$, with:

$$\mathrm{d_i} = \begin{cases} 0 \; if \; C_i.\mathrm{B} \neq 0 \\ j \; if \; C_i.\mathrm{B} = 0 \end{cases}$$

Where j is the largest integer from $\{1, 2, \ldots n-1\}$ such that $C_i.\mathrm{A}^{\mathrm{d_i}}.\mathrm{B} = 0$ for $k = 0, 1, \ldots j-1$.

Once $\mathrm{d_i}$ and $\mathrm{D_i}$ are calculated, the system is decoupled by the following matrices F and G [26]:

$$\begin{cases} F = -D^{-1}.\tilde{A} \\ G = D^{-1} \end{cases}$$

Where:

$$D = \begin{bmatrix} D_1 \\ D_2 \\ D_3 \end{bmatrix} and \tilde{A} = \begin{bmatrix} C_1 A^{d_1+1} \\ C_2 A^{d_2+1} \\ C_3 A^{d_3+1} \end{bmatrix}$$

And the i[th] output is the $(d_i + 1)$-fold integral of the i[th] input.

3.2 Application to the flexible manipulator

For the flexible manipulator, new inputs to the system are going to be defined in order have a decoupled system.

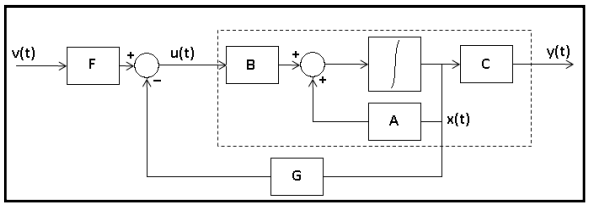

Figure3.1. State feedback decoupling scheme

The initial input vector is :

$$u = [u_m(t) \;\; u_p^1(t) \;\; u_p^2(t)]_{1\times 3}^T$$

And the state vector is :

$$x = [\theta \;\; a_1 \; a_2 \;\; \dot{\theta} \;\; \dot{a}_1 \; \dot{a}_2]^T$$

The control law used is defined as:

$$u = F.x(t) + G.v(t)$$
$$= F.x(t) + G[v_m(t) \;\; v_p^1(t) \;\; v_p^2(t)]_{1\times 3}^T$$

Calculation results on:

$$\mathrm{d_i} = 1 \text{ for i} = 1,2 \text{ and } 3$$

So, matrices $D$and $\tilde{A}$ are given by:

$$D = C.A.B \;\; and \;\; \tilde{A} = C.A^2$$

And each output of the system is going to be the double integral of its appropriate control input.

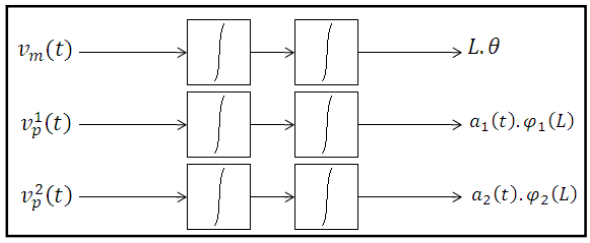

Figure3.2. Decoupled system

4. FIRST ORDER SLIDING MODE CONTROL

Since the flexible manipulator has been decoupled into three, single-input single-output second order, slightly independent systems, the first order sliding mode controller can be easily formulated.

1.1. Controller formulation

Considering the decoupled model of the flexible one-link manipulator, the system model is:

$$\begin{cases} \ddot{\theta} = v_m(t) \\ \ddot{a}_1 = v_p^1(t) \\ \ddot{a}_2 = v_p^2(t) \end{cases}$$

The tracking errors for state variables are defined as:

$$\begin{cases} e_\theta = \theta - \theta_d \\ e_{a_1} = a_1 - a_{1d} \\ e_{a_2} = a_2 - a_{2d} \end{cases}$$

The crucial and the most important step of SMC design is the construction of the sliding surface $s(t)$, also called sliding function.

A sliding mode is said “first order sliding mode” if and only if $s(t) = 0$ and $s(t)\dot{s}(t) < 0$. The inequality $s(t)\dot{s}(t) < 0$ is the fundamental condition for sliding mode. The aim of the first-order sliding mode control is to force the state (error) to move on the switching surface $s(t) = 0$.

The sliding surface, in the traditional SMC depends on the tracking error $e(t)$ and its derivative(s) as [19]:

$$s(t) = \left(\lambda_c + \frac{d}{dt}\right)^{n-1} e(t)$$

where n denotes order of uncontrolled system and λ_c is a positive constant.

If the system concerned is assumed to be of second-order, the first time derivative of the sliding surface is:

$$\dot{s}(t) = \lambda_c \dot{e}(t) + \ddot{e}(t)$$

The second time derivative of the error, ë(t) relatively to each state, can be written in terms of the plant new inputs as:

$$\begin{cases} \ddot{e}_\theta = \ddot{\theta} - \ddot{\theta}_d = v_m(t) \\ \ddot{e}_{a_1} = \ddot{a}_1 - \ddot{a}_{1d} = v_p^1(t) \\ \ddot{e}_{a_2} = \ddot{a}_2 - \ddot{a}_{2d} = v_p^2(t) \end{cases}$$

And, the switching surfaces may be defined as:

$$\begin{cases} s_\theta(t) = \lambda_\theta e_\theta(t) + \dot{e}_\theta(t) \\ s_{a_1}(t) = \lambda_{a_1} e_{a_1}(t) + \dot{e}_{a_1}(t) \\ s_{a_2}(t) = \lambda_{a_2} e_{a_2}(t) + \dot{e}_{a_2}(t) \end{cases}$$

The control input can be given as[19]:

$$u(t) = v_{eq}(t) + v_{sw}(t)$$

where $v_{eq}(t)$ and $v_{sw}(t)$ are the equivalent control and the switching control, respectively.

The equivalent control, $v_{eq}(t)$, proposed by Utkin[25], is based on the nominal (estimated) plant parameters and provides the main control action. The switching control, $v_{sw}(t)$, ensures the discontinuity of the control law across sliding surface, supplying additional control to account for the presence of matched disturbances and unmodeled dynamics.
If the initial error is not on the sliding surface $s(t)$ due to parameter variations and disturbances, the controller must be designed such that it can drive the error to the sliding surface. The error under the condition that will move toward and reach the sliding surface is said to be on the reaching phase.

4.1 Equivalent control

The equivalent control approach is defined as the smooth feedback control law that locally sustains the evolution of the error ideally restricted to the smooth sliding surface $s(t)$ when the initial error of the system is located precisely on it. This control allows an asymptotic convergence of the sliding function to zero according to a desired dynamic and the control forces the system to evolve on the sliding surface.

Thus, in the design of sliding mode controllers, an equivalent control is first given so that the states can stay on sliding surface. Consequently, the system dynamics in sliding motion is independent of the original system and a stable equivalent control system is achieved.

The equivalent control is obtained when $\dot{s}(t) = 0$, which is the necessary condition for the tracking error to remain on the sliding surface.

Now, an equivalent control for the three states can be defined:

$$\begin{cases} \dot{s}_\theta(t) = \lambda_\theta \dot{e}_\theta(t) + \ddot{e}_\theta(t) = 0 \Leftrightarrow v_{eq}^{\theta}(t) = -\lambda_\theta \dot{e}_\theta(t) \\ \dot{s}_{a_1}(t) = \lambda_{a_1} \dot{e}_{a_1}(t) + \ddot{e}_{a_1}(t) = 0 \Leftrightarrow v_{eq}^{a_1}(t) = -\lambda_{a_1} \dot{e}_{a_1}(t) \\ \dot{s}_{a_2}(t) = \lambda_{a_2} \dot{e}_{a_2}(t) + \ddot{e}_{a_2}(t) = 0 \Leftrightarrow v_{eq}^{a_2}(t) = -\lambda_{a_2} \dot{e}_{a_2}(t) \end{cases}$$

4.2 Switching control

The switching control is introduced as[19]:

$$v_{sw}(t) = -k.\,sign(s(t))$$

where k is a positive constant, chosen to dominate the matching uncertainties, and sign(.) denotes sign function defined by:

$$sign(s) = \begin{cases} 1 \;\; if \; s > 0 \\ 0 \;\; is \;\; s = 0 \\ -1 \; if \; s < 0 \end{cases}$$

Consequently, the control laws for the three states are given as:

$$v_m(t) = v_{eq}^{\theta}(t) + v_{sw}^{\theta}(t) = -k_\theta sign(s_\theta) - \lambda_\theta \dot{e}_\theta(t)$$
$$v_p^1(t) = v_{eq}^{a_1}(t) + v_{sw}^{a_1}(t) = -k_{a_1} sign(s_{a_1}) - \lambda_{a_1} \dot{e}_{a_1}(t)$$
$$v_p^2(t) = v_{eq}^{a_2}(t) + v_{sw}^{a_2}(t) = -k_{a_2} sign(s_{a_2}) - \lambda_{a_2} \dot{e}_{a_2}(t)$$

5. SIMULATION AND RESULTS

This section illustrates the results of the simulations conducted on the flexible beam that is solidly coupled to the shaft of a servomotor.

The motor is rotated and controlled to an angular set-point using a sliding mode controller.

During rotation, the beam's vibrations are suppressed using piezoceramic actuators until set-point of the joint angle has been completed.
First, results are illustrated when only joint angle is controlled. The single-input single-output (SISO) controller uses $v_m(t)$ as the control variable while the controlled variable is θ.
Then, the piezoceramic actuators are used to diminish the beam vibrations during the rotation. The effect of each mode of vibration will be controlled separately. The single-input single-output (SISO) controllers uses respectively $v_p^1(t)$ and $v_p^2(t)$ as the control variables for the manipulated variables a_1 and a_2.

5.1 Joint angle control

The Joint angle set-point is 45°, and the control law is given by:

$$v_m(t) = v_{eq}^{\theta}(t) + v_{sw}^{\theta}(t) = -k_\theta sign(s_\theta) - \lambda_\theta \dot{e}_\theta(t)$$

The simulation illustrate the effect of the parameters: k_θ and λ_θ.

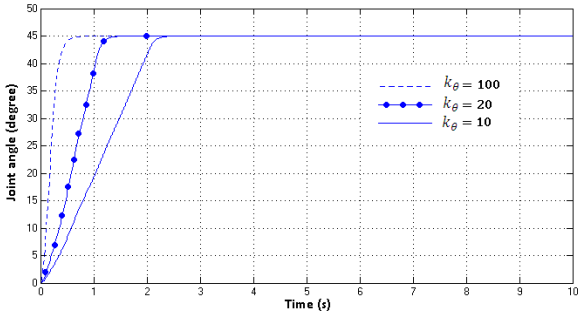

Figure 5.1: Joint angle sliding mode control evaluation of the parameter k_θ (λ_θ=10)

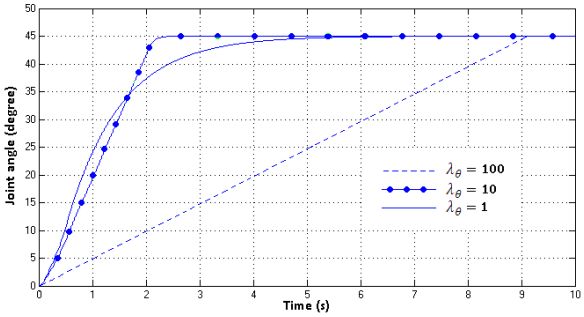

Figure 5.2: Joint angle sliding mode control evaluation of the parameter λ_θ (k_θ=10)

The response of the system comes to be faster as the parameter k_θ increases.
The parameter λ_θ doesn't have an important effect on the system acceleration because its influence start once the response reach the switching surface and not during the reaching phase.
The equivalent control input to the servomotor is very oscillatory as it's illustrated in Figure 5.3.

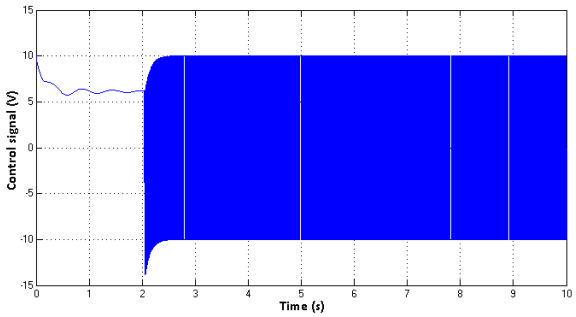

Figure 5.3: Joint angle sliding mode control evaluation of the control signal sent to the servomotor (k_θ=10 and λ_θ=10)

The figures 5.4 and 5.5 illustrate the sliding surface and the phase plane respectively.

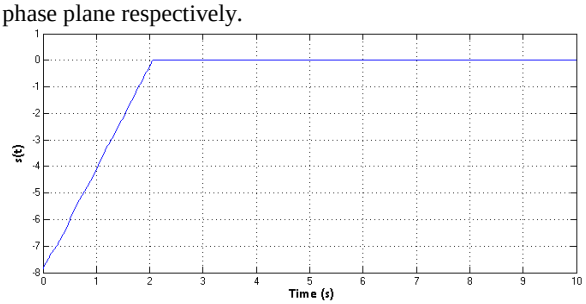

Figure 5.4: Sliding surface s(t)

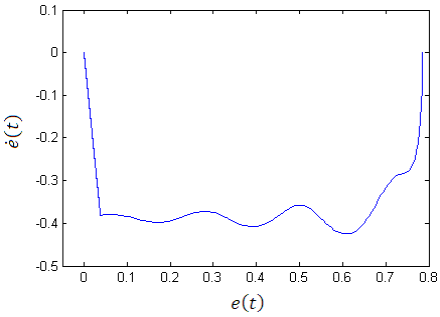

Figure 5.5: The phase plane $e(t)$ and $\dot{e}(t)$

The sliding mode is in the reaching phase up to 2s and then arrives to the sliding phase. The error and its first derivative comes to zero at steady-state conditions.

5.2 Piezoelectric actuators control

The tip displacement set-points are chosen to be equal to 0.1mm and 0.01mm respectively for the first and second mode contributions, and the control inputs send to the piezoelectric actuators are :

$$v_p^1(t) = v_{eq}^{a_1}(t) + v_{sw}^{a_1}(t) = -k_{a_1} sign(s_{a_1}) - \lambda_{a_1}\dot{e}_{a_1}(t)$$
$$v_p^2(t) = v_{eq}^{a_2}(t) + v_{sw}^{a_2}(t) = -k_{a_2} sign(s_{a_2}) - \lambda_{a_2}\dot{e}_{a_2}(t)$$

Similarly to the joint angle control, the consequences of manipulating $v_p^1(t)$ and $v_p^2(t)$ on the first and second mode contributions to the tip displacement. are illustrated.

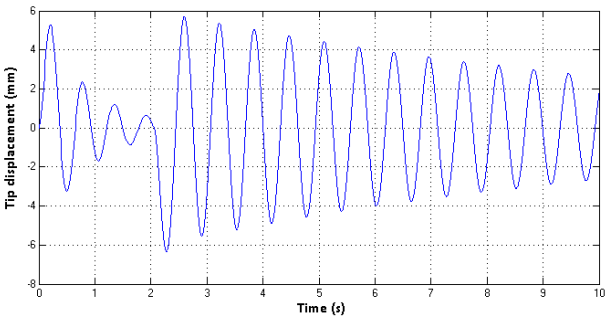

Figure 5.6: First mode contribution to the tip displacement (only joint angle is controlled with k_θ=10 and λ_θ=10)

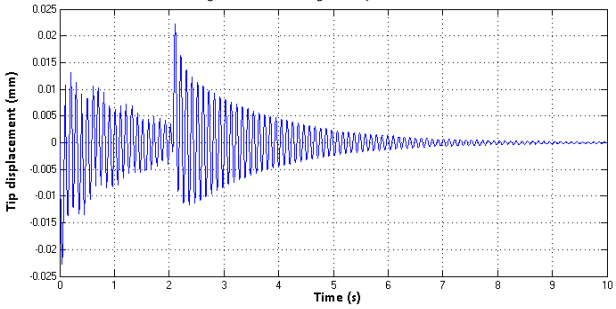

Figure 5.7: Second mode contribution to the tip displacement (only joint angle is controlled with k_θ=10 and λ_θ=10)

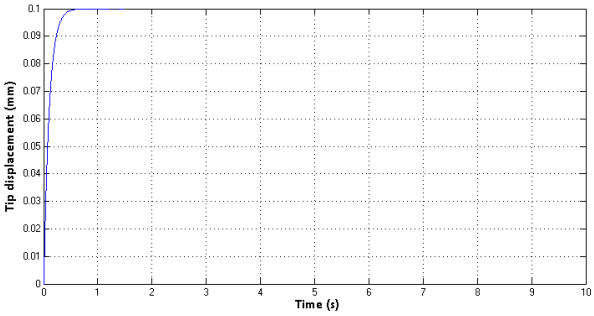

Figure 5.8: First mode contribution to the tip displacement (PZT is controlled with k_{a_1}= 0.1 and λ_{a_1}=10)

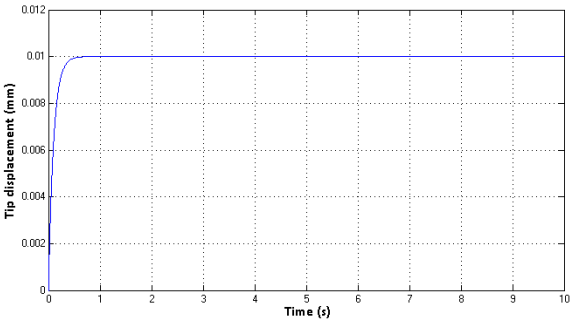

Figure 5.9: Second mode contribution to the tip displacement (PZT is controlled with k_{a_2}= 0.01 and λ_{a_2}=10)

It's clear that the objective is reached. The tip displacements due to vibrations of 1st and 2nd mode are reduced to 0.1mm and 0.01mm respectively.

The problem is on the control signals sent to the piezoelectric actuators, and it's illustrated in Figures 5.10 and 5.11.

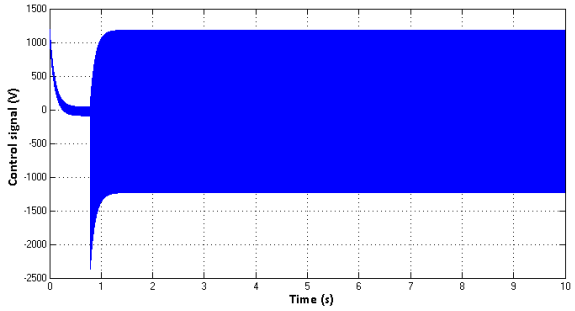

Figure 5.10: Control signal sent to the 1st PZT

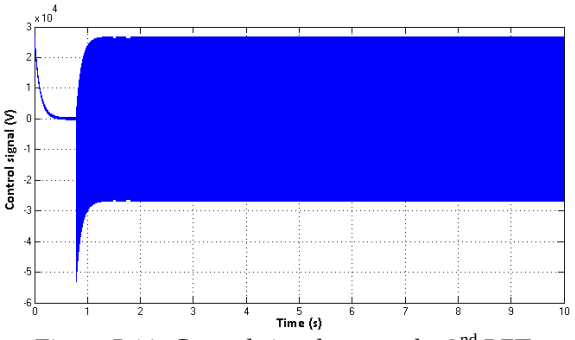

Figure 5.11: Control signal sent to the 2nd PZT

In addition to the fact that they are very oscillatory, control signal reaches very high values that can't be supported by piezoelectric actuators.

6. CONCLUSIONS

State space equations of the flexible manipulator, that describe the rigid and flexible motions, were expressed using the Euler–Lagrange formulation. The flexible displacement was calculated using modal analysis and beam theory.

The piezoelectric actuators effect, on the manipulator model, was properly introduced via the stiffness and force matrices.

The system was decoupled into three independent single-input single-output systems using a state feedback decoupling scheme. The advantage of this strategy was to provide direct control on proper modes of vibration contributions to the flexible manipulator tip displacement.

A sliding mode controller was, then, implemented for each one of the three independent systems. Although the control signal was very oscillatory and of higher magnitude, and no comparisons to other controllers were conducted, this method of control has successfully demonstrated its ability to perfectly control the rigid body rotation. It has also proved a good vibration decreasing within a very satisfying time.

Both, for decoupling and for controlling the system, state variables should be measured. Those measures were not discussed in this paper. However; in practice, the modal coordinates are well estimated using piezoelectric films as sensors, and the joint angle is simply measured using a potentiometer.

REFERENCES

[1] Recent advances in sensing and control of flexible structures via piezoelectric materials.
Sunar M, Rao SS. Appl Mech Rev 999;52(10):1–16.

[2] Modeling of an active constrained layer damper proc.
Plump JM, Hubbard Jr JE. In: 12th intl congress on acoustics, Toronto, Canada, 1986; #D4-1.

[3] Distributed piezoelectric-polymer active vibration control of a cantilever beam.
Bailey T, Hubbard Jr JE. J Guidance Control Dynam 1985;8(5):605–11.

[4] Performance of an active control system with piezoelectric actuators.
Baz A, Poh S. J Vib Control 1988;126(2):327–43.

[5] Control of a miniature gripper driven by piezoceramic bimorph cells.
Chonan S, Jiang ZW, Sakuma S. Force J Adv Automat Technol, 1994;6:247–54.

[6] Variable structure adaptive control of a cantilever beam using piezoelectric actuator.
Yim W, Singh SN. J Vib Control, 2000; 6:1029–43.

[7] Identification and control of a benchmark flexible structure using piezoelectric actuators and sensors.
Lin CL, Lee GP, Liu VT. J Vib Control, 2003;9(12):1401–20.

[8] Robust control for structural systems with parametric and unstructured uncertainties.
Wang S, Yeh H, Roschke PN. J Vib Control, 2001;7:753–72.

[9] A robust disturbance rejection method for uncertain flexible mechanical vibrating systems under persistent excitation.
Zheng LA. J Vib Control, 2004;10(3):342–57.

[10] Optimal design of number and locations of actuators in active vibration control of a space truss.
Yam LH, Yan YJ. Smart Mater Struct, 2002;11:496–503.

[11] Predictive control of flexible structures.
Wang R, Hassan M, Dubay R. In: Flexible automation & intelligent manufacturing conference, Toronto, Ontario, 2004. p. 98–104.

[12] Vibration control of flexible structure using smart materials.
Bravo R. PhD dissertation. McMaster University, Canada, 2000.

[13] The synthesis of linear multivariable systems by state variable feedback
B. S. MORGAN, JR. Proc. 1964 JACC, Stanford, California, pp. 468-472.
[14] Decoupling of multivariable systems by means of statefeedback
Z.V. REKASIUS. Proc. Third Allerton Conference on Circuit and System Theory, Monticello, Illinois, 1965, pp. 439-448.
[15] On the decoupling of multivariable systems.
P. L. F,LB ,ND W. A. WOLOVICn, Proc. 1967 JACC, Philadelphia, Pennsylvania, pp. 791-796.
[16] Second order sliding mode control of vehicles with distributed collision avoidance capabilities.
Ferrara A, Vecchico C. Mechatronics, 2009; 19:471_7.
[17] Sliding mode control of quadruple tank process.
Biswas PP, Srivastava R, Ray S, Samanta AN. Mechatronics 2009;19:548_61.
[18] High-order sliding control of mechanical systems: Theory and experiments.
Cavallo A, Natale C. Control Eng Pract, 2004; 12:1139_49.
[19] Applied nonlinear control.
Slotine JJ, Li W. Englewood Cliffs (New Jersey): Prentice Hall Inc.; 1991.
[20] Regulation of a one-link flexible robot arm using sliding-mode technique
K.S. Yeung; Y.P. Chen, International Journal of Control, 1989.
[21] Active vibration control of a flexible beam using a non-collocated acceleration sensor and piezoelectric patch actuator
Z Qiu, J Han, X Zhang, Y Wang – Journal of sound and vibration, 2009.
[22]A PZT actuator control of a single-link flexible manipulator based on linear velocity feedback and actuator placement
DSun, JK Mills, J Shan, Mechatronics, 2004.
[23] Sliding order and sliding accuracy in sliding mode control.
Levant A. Internat J Control, 1993; 58:1247_63.
[24] Composite modeling of flexible structures with bonded piezoelectric film actuators and sensors.
Vaz A. IEEE Trans Intrum Measur1998; 24(2):513–20.
[25] Sliding modes in optimization and control problems.
Utkin VI. New York: Springer-Verlag; 1992.
[26] The decoupling of multivariable systems by state feedback .
Elmer, G. Gilbert, SIAM J. CONTROL Vol. 7, No. 1, February 1969